An Efficiency Model For the Reflection Gratings on XMM's RGS

Jean Cottam, Steven Kahn, Andrew Rasmussen, Joshua Spodek
Columbia Astrophysics Laboratory

Frits Paerels
Space Research Organization of the Netherlands

ABSTRACT

We present a model of the efficiency for the reflection gratings on XMM's RGS over the full instrumental range of wavelengths, orders and incident angles. The model has been developed using the full vector solution to Maxwell's equations for the set of boundary conditions describing the grating profile and modified using scalar theory to account for both scattering effects due to incoherent noise on the surface of the grating and a redistribution of light from low spectral orders into higher orders due to a coherent modulation on the groove profile. This model reproduces the efficiency measurements to approximately 5% error over most of the band.

1. Introduction

The effective area of the Reflection Grating Spectrometer (RGS) on XMM is a product of the telescope effective area, the efficiency of the Reflection Grating Array (RGA), the CCD efficiency, and geometric factors in the instrument alignment (refer to "The XMM/RGS Effective Area" by C. de Vries et al.). While the determination of the telescope effective area and the CCD efficiency are fairly straightforward, an exact calculation of the reflectivity of a grating in the X-ray region presents difficulties not normally encountered in longer wavelength regimes.

In the past, reflectivities have been estimated empirically from limited sets of calibration data. Since it is physically impossible to sufficiently sample the full range of wavelength, incident angle and spectral orders which will be observed with XMM, it is necessary to create a physical model for the efficiency of the gratings.

2. Scalar Theory vs. Full Electromagnetic Solution

Previous attempts to model the efficiency used scalar diffraction theory, which assumes perfect reflectivity of the surface and ignores the vector character of the radiation fields. While this approximation is acceptable in the optical and UV regions, it breaks down in the X-ray region where the absorption of light becomes significant and strongly angle dependent. Instead, we solve Maxwell's equations for the grating problem explicitly. Neviere has developed a numerical solution to Maxwell's equations subject to the appropriate boundary conditions (Breidne and Neviere, 1984). We adopted his approach and implemented a numerical scheme to solve the difference equations. Figure 2 shows the difference between the scalar theory and the EM solution for the nominal RGS grating profile shown in Figure 1.

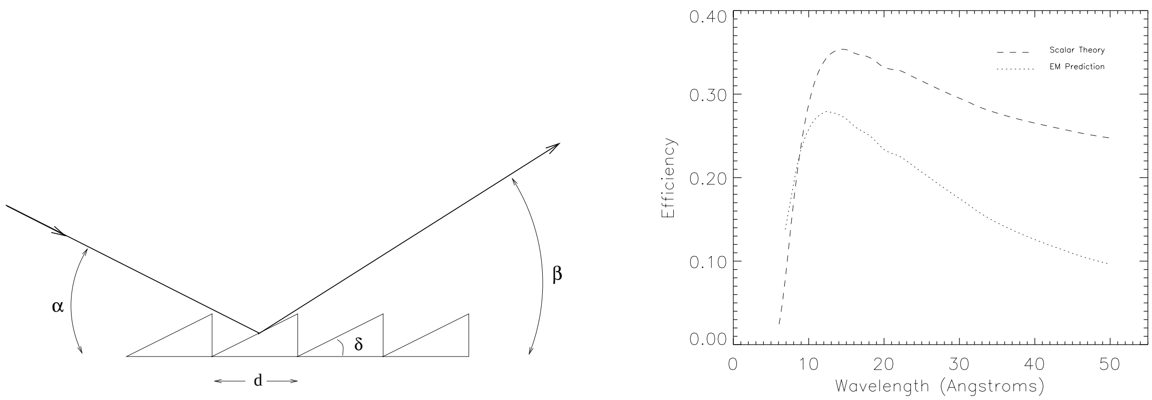

Fig. 1.— Left: The RGA nominal grating with a perfect sawtooth profile of blaze angle δ. α is the angle of the incident beam with respect to the grating surface, d is the grating line spacing, and β is the dispersion angle calculated according to the diffraction equation, $m\lambda = d(\cos\beta - \cos\alpha)$, with spectral orders $m = 0, -1, -2$, etc. Right: A comparison between the scalar theory prediction (dashed line) and the EM prediction (dotted line) for reflectivity as a function of wavelength at first order for the nominal RGS grating profile.

3. Model Parameters

Since the EM efficiency of the nominal grating profile fails to reproduce the measured efficiency, we have included the following parameters in the efficiency model. The groove profile constitutes the boundary conditions for the EM calculation. It is parameterized by the blaze angle and the amplitude of a bump on the surface of the groove (evident in STM images of the grating). A coherent modulation on the grating surface is included as a described below and parameterized by the coherence length and average rms surface roughness of the modulation. Incoherent scattering is calculated according to the scalar theory scattering formulas described below and parameterized by the coherence length and average rms surface roughness of the noise. Finally, we have included a hydrocarbon contamination layer on the surface of the grating, modelled by a thin carbon absorption layer.

4. Coherent Modulation

There is evidence of a roughness on the surface of the grating which is repeated exactly from groove to groove. As this is difficult to implement in the EM calculation, we have modelled this coherent modulation according to the following heuristic argument: Since a grating with a coherent roughness is equivalent to the convolution of a smooth groove with a rough plane, the efficiency pattern for such a grating should be equivalent to the convolution of the efficiency pattern of a smooth groove (given by the EM calculation) with the light distribution profile of a noisy plane (given by scalar scattering theory).

We have performed this convolution using the following heuristic formula:

$$Eff_{\rm m} = EM_{\rm m}(1 - F) + Rf_{\rm m}$$

Where $EM_{\rm m}$ is the EM calculated efficiency and $f_{\rm m}$ is the fraction of scattered light for spectral order m, and where R and F are the total reflectivity and total scattered light summed over all spectral orders. This process, shown in Figure 2, conserves the total amount of light, while it increases the fraction of light in higher spectral orders and decreases the amount of light in lower spectral orders relative to the original EM calcuation.

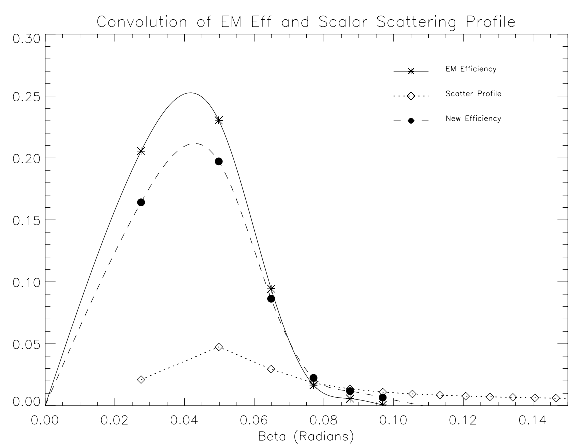

Fig. 2.— The convolution of the EM efficiency prediction with the scalar theory scattering profile. The stars connected by the solid line show the EM efficiency, the envelope for the efficiency of a perfect grating. The diamonds connected by the dotted line show the scalar theory scattering profile, the envelope for the rough flat surface. Combining the two results in the dots connected by the dashed line.

5. Incoherent Scattering

Incoherent noise on the grating scatters light into the regions between the spectral orders lowering the measured efficiency. Scalar scattering theory gives the following expressions to describe the distribution of light:

$$\frac{1}{\eta_{\rm m}}\frac{d\eta_{\rm m}}{d\beta} = \frac{(\sin\alpha + \sin\beta)^4}{(\sin\alpha + \sin\beta_{\rm m})^2}\sin\beta_{\rm m} k^3 W(p),$$

$$W(p) = \frac{l\sigma^2}{\pi}\int_{-\infty}^{+\infty}\frac{dp}{1+l^2p^2},$$

$$p = k(\cos\beta_{\rm m} - \cos\beta).$$

There are only two parameters in these expressions, the coherent length, l, and the rms surface roughness, σ. Inter-order scans performed at Nevis Labs allow us to fit these parameters with the following results. For all gratings, the coherence length is given by $l_{\rm incoherent} = 1.0\mu$m. The rms roughness varies by grating from $\sigma_{\rm incoherent} = 8$Å to 15Å.

6. Calibration Data

The calibration data for the efficiency of the RGS gratings comes from two facilities. The BESSY facility in Berlin has a synchrotron beam which provides continuous energy coverage from 200 eV to 2000 eV. Four gratings have been calibrated there for spectal orders m=0,-1,-2 at nominal incidence. The Longbeam facility at Columbia University's Nevis Laboratory provides single target measurements at CuL (13.34Å), AlK (8.34Å), FeL(17.59Å), and OK(23.63Å) for all gratings used in the RGS over a range of orders and icident angles. For the purposes of constraining the efficiency model the following calibration data have been used: Eff(λ) at $\alpha = 1.58°$ for $m = -1, -2$, Eff(α) at CuL for $m = -1, -2$, Eff(m) at $\alpha = 1.58°$ for CuL and AlK, and Eff(β) at $\alpha = 1.58°$ for CuL.

7. Efficiency Model

The efficiency model, optimized for all data sets, has the following parameters: the groove is described by a 0.78° blaze angle with a 35Å bump. The coherent modulation is described by a coherence length of 0.29μm and a rms surface roughness of 15Å. There is a hydrocarbon contamination layer of 1Å on the surface of the grating.

The comparisons in Figures 3, 4, 5, and 6 show an excellent agreement between the modelled efficiency and the measurement data including the inter-order scattering levels. Residual errors are less than 5% for first order and less than 8% for second order over most of the range of wavelengths and incident angles. In the region of low wavelength the model is less exact with errors of $\sim$ 20% at wavelengths below 9Å. The model overpredicts efficiencies for spectral orders above and including $m = -3$.

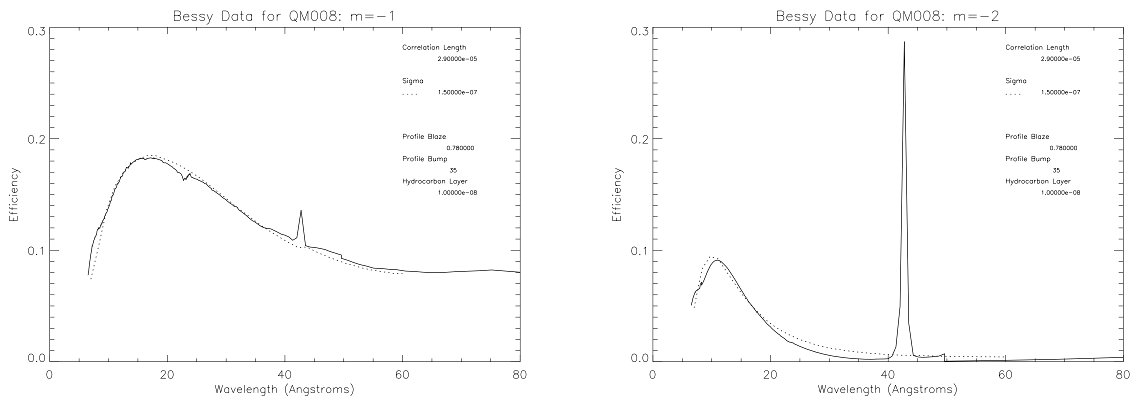

Fig. 3.— A comparison between the calibration data taken at BESSY (solid line) and the efficiency model prediction (dotted line) for efficiency as a function of wavelength at first order (left) and second order (right). The percentage error is less than 5% in the operating region for both first order ($\lambda_{\max} = 35$Å) and second order ($\lambda_{\max} = 17$Å) except for wavelengths below 9Å. The spikes in the data are due to carbon contamination on the BESSY monochromator and may be ignored.

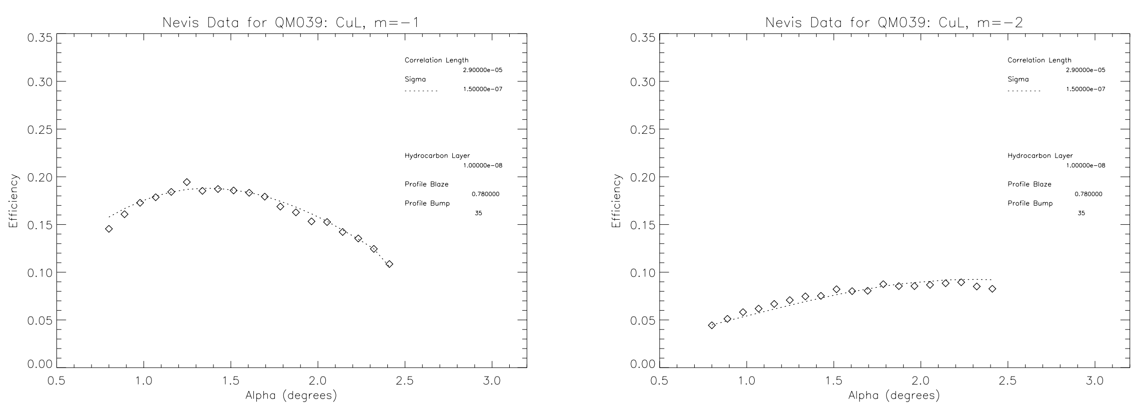

Fig. 4.— A comparison between the calibration data taken at Nevis (diamonds) and the efficiency model prediction (dotted line) for efficiency as a function of angle at CuL for first order (left) and second order (right). The percentage error is less than 5% for first order and less then 8% for second order in the operating regions of the instrument ($1^\circ < \alpha < 2^\circ$).

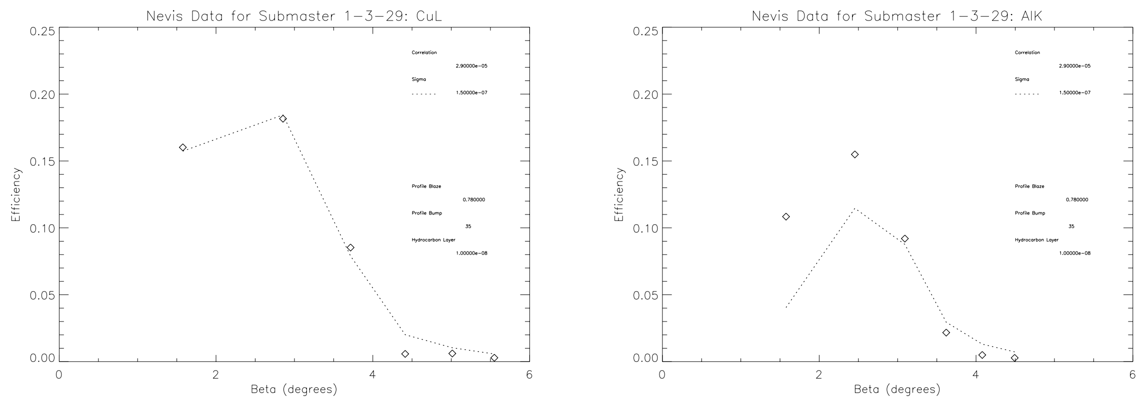

Fig. 5.— A comparison between the calibration data taken at Nevis (diamonds) and the efficiency model prediction (dotted line) for efficiency as a function of spectral order at CuL (left) and AlK (right). The percentage error is less than 7% for low orders of CuL and about 25% for AlK. Spectral orders above and including third order are overpredicted for all wavelengths, however for most wavelengths these orders lie outside of the range of the instrument.

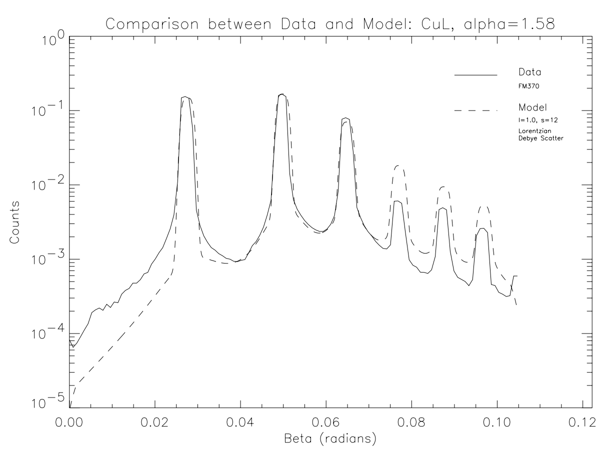

Fig. 6.— A comparison between the inter-order efficiency scan taken at Nevis (solid line) and the efficiency model prediction (dashed line) for CuL at nominal incidence. For low spectral orders the incoherent scattering levels and profile distribtuion are in excellent agreement with the data. At higher orders the known overprediction of the efficiency model incorrectly normalizes the profiles.